



Cite this: *Chem. Commun.*, 2016, 52, 4305

Received 22nd December 2015,
Accepted 22nd February 2016

DOI: 10.1039/c5cc10496c

www.rsc.org/chemcomm

Dramatic mechanistic switch in Sn/Au^I group exchanges: transmetalation vs. oxidative addition†

D. Carrasco,^a M. García-Melchor,^{*b} J. A. Casares^{*a} and P. Espinet^{*a}

The mechanism of Ph/X exchange in reactions involving SnPhⁿBu₃ and [AuXL] complexes switches dramatically from the usual concerted mechanism involving Ar/X mixed bridges when X = Cl, to an unexpected oxidative addition/reductive elimination pathway via an Au^{III} intermediate when X = vinyl.

Whereas organic-group/halide exchanges operating in cross-coupling catalysis have been studied in detail,¹ transmetalations exchanging two carbon groups between metals, often involved in bimetallic catalysis and in formation of unwanted homocoupling products,² are very little studied.

Recently, transmetalation between gold complexes and organotin derivatives has drawn attention due to its occurrence in multi-metallic catalytic processes. For example, we have shown that Au^I complexes co-catalyze the coupling of bulky stannanes in the gold co-catalyzed Stille reaction. In this new process a Sn/Au/Pd double transmetalation occurs through successive Sn/Au and Au/Pd transition states with a much lower activation energy than the direct Sn/Pd transmetalation, which allows for coupling of bulky groups.³ Blum has studied the vinyl exchange between gold and tin in the Pd/Au co-catalyzed carbostannylation of alkynes.⁴ The gold-catalyzed cycloisomerization/stannylation cascade reaction of 1,6-diyne-4-en-3-ols using 2-(furyl)Sn(*n*-Bu)₃ as the primary source of stannane, and leading to stannyl naphthalenes has been reported by Chen.⁵ Bourissou has communicated examples of transmetalation from vinyl gold complexes to SnBu₃(OTf) in the presence of PPh₃.⁶ Furthermore, some of these transmetalations in Au/Pd/Sn systems have been computationally calculated.^{3a,7} In this work we combine experiments and DFT calculations to study the mechanisms of Sn/Au transmetalation in which a Ph group is exchanged by a halogen or by a vinyl group.

Unexpectedly, we find a dramatic mechanistic switch from the first to the second transmetalation process somehow representing the subtle connection between the concepts of acid–base interaction and oxidation–reduction.

First, the thermodynamics of X for R exchange between Au^I and Sn was experimentally studied in THF for a number of cases: X = I, Cl, vinyl; L = PMe₃, PCy₃, PPh₃; R = Ph, C₆Cl₃F₂, C₆F₅, 2Me-naphthyl (eqn (1)).⁸ The exchange reactions are reasonably fast for X = halide, and the corresponding equilibria can be reached at 303 K. For X = I, they are strongly shifted to the right, except for R = 3,5-C₆Cl₂F₃ and C₆F₅; these are slightly shifted to the left due to the stronger Au–C bond for perhaloaryl groups compared to non-halogenated aryls. For X = Cl the equilibria are much more balanced due to the high energy of the Sn–Cl bond, which makes the equilibrium displacement to the right less favourable.^{3a} For X = vinyl, the C_{aryl}/C_{alkyl} exchange is too slow at room temperature, and equilibration is only achieved reasonably fast at 323 K, when an equilibrium slightly displaced to the left is produced.



The reaction rates from left to right of eqn (1), for Ph/Cl exchanges at 303 K with L = PCy₃, PMe₃, and PPh₃ are, respectively, 3.4 × 10^{−4}, 5.1 × 10^{−4}, and 9.4 × 10^{−5} L mol^{−1} s^{−1}. The modest dependence on the phosphine ligand suggests that phosphine dissociation during the Ar/X exchange reaction does not occur and the variations are only due to the electronic differences of the phosphines as coordinating ligands.

With these data in hand, the exchanges between [AuPh(PMe₃)] and SnXBu₃ with X = Cl and vinyl were chosen for detailed study, in view of the somewhat unexpectedly large rate difference observed between them. These reactions were monitored in THF and in toluene solutions, using ³¹P NMR.

The solutions of SnClBu₃ and [AuPh(PMe₃)] in THF are non-conducting, supporting that the Cl ligand remains coordinated to one metal centre, at least, throughout the reaction. The study of the Ph/Cl transmetalation, using Sn:Au = 20:1 in order to simplify the handling of data and to ensure that the equilibrium

^a IU CINQUIMA/Química Inorgánica, Facultad de Ciencias, Universidad de Valladolid, 47071 Valladolid, Spain. E-mail: espinet@qi.uva.es, casares@qi.uva.es

^b SUNCAT Center for Interface Science and Catalysis, Department of Chemical Engineering, Stanford University, Stanford, CA 94305, USA

† Electronic supplementary information (ESI) available: Experimental section and computational details (40 pages). See DOI: 10.1039/c5cc10496c



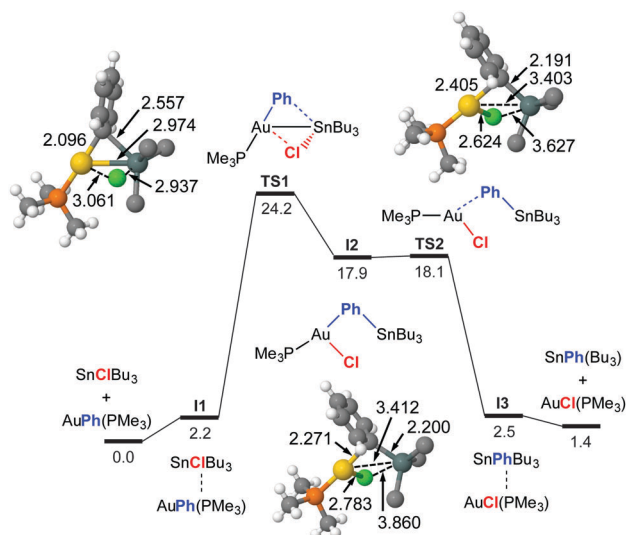


Fig. 1 Calculated Gibbs energy profile in THF (kcal mol⁻¹, at 323 K and $p = 301$ atm, bond distances in Å) for the rearrangement of [AuPh(PMe₃)] and SnClBu₃ into [AuCl(PMe₃)] and SnPhBu₃. The *n*-Bu moieties have been simplified to C in the figure. Color code: C (gray), H (white), P (orange), Cl (light green), Au (gold), Sn (dark green). I2 might not be a real intermediate.

is established in a reasonable time, affords $K_{\text{eq}} = 1.1$ at 298 K. Kinetic experiments at 303 K show that the reaction is first order in [AuPh(PMe₃)].⁸ The exchange rates measured in the temperature range 250–330 K afford the activation parameters $\Delta H^\ddagger = 27(\pm 2)$ kJ mol⁻¹, $\Delta S^\ddagger = -223(\pm 23)$ J K⁻¹ mol⁻¹, $\Delta G^\ddagger_{298} = 22.3$ kcal mol⁻¹. For comparison with experiments and calculations to come, for this reaction $\Delta G^\ddagger_{323} = 23.7$ kcal mol⁻¹. The strongly negative ΔS^\ddagger value clearly supports an associative exchange process. The same reaction was also studied in toluene, resulting in a very similar activation Gibbs energy ($\Delta G^\ddagger_{298} = 22.0$ kcal mol⁻¹), which discards the possible participation of THF as coordinating agent in the first transmetalation.

The TS1 energy ($\Delta G^\ddagger_{323} = 24.2$ kcal mol⁻¹) in Fig. 1 matches well the experimental activation energy and the DFT profile predicts a fairly balanced equilibrium, as observed experimentally. The calculations also coincide with the experimental result that the phosphine ligand remains coordinated to gold along the reaction pathway. The mechanism basically consists in a double group exchange *via* single- or double-bridged intermediates or transition states, as typically found in Pd. At variance with Pd^{II}, the transmetalation involving Au^I does not require releasing the ancillary ligand, and the coordination number of gold increases from 2 to 3 at the transition state.

The Ph/vinyl exchange was also studied using a 20 fold proportion of Sn(vinyl)Bu₃ to produce [Au(vinyl)(PMe₃)] and SnPhBu₃. As commented above, no conversion was observed at room temperature, but it took place at a low rate of $1.7 (\pm 0.2) \times 10^{-6}$ L mol⁻¹ s⁻¹ when heated 323 K ($\Delta G^\ddagger_{323} = 27.5$ kcal mol⁻¹). A wide enough temperature range for measuring ΔH^\ddagger and ΔS^\ddagger was not accessible due to partial decomposition to gold upon heating above 333 K, and too slow reaction below 313 K.

For this exchange DFT calculations prove that the double group exchange mechanism *via* bridged intermediates, proposed for

X = Cl, has to be discarded for X = vinyl because it has a very high energetic barrier (42.1 kcal mol⁻¹) at the rate-determining step.⁸ Calculations provide instead a reasonable highly symmetrical alternative pathway, much lower in energy, which matches well the experimental ΔG^\ddagger value and uncovers a dramatic mechanistic change (Fig. 3). It involves the oxidative addition of the Sn–C_{vinyl} bond to Au *via* TS3, to produce *trans*-[Au(SnBu₃)(Ph)(vinyl)(PPh₃)] (I5), a square-planar gold intermediate from which the Sn–C_{Ph} or Sn–C_{vinyl} reductive elimination *via* TS4 can give rise to the respective Au^I and Sn products. The calculated ΔG^\ddagger_{323} values are 28.6 kcal mol⁻¹ starting from [AuPh(PMe₃)], and 28.9 starting from [Au(vinyl)(PMe₃)]. This result prompted us to carry out, as caution, a calculation of the TS energy in an oxidative addition/reductive elimination pathway for Ph/Cl exchange (see ESI,[†] Fig. S6), which afforded an energetic barrier of 34.2 kcal mol⁻¹, confirming its unlikelihood.

Looking at Fig. 1 and 2, it catches the eye that the closely linear arrangement (P–Au–X $\approx 180^\circ$) present in all the starting [AuX(PMe₃)] complexes is very differently altered in the transition states. More specifically, TS3 shows a large alteration (P–Au–Ph = 116°) at the initial interaction, while the change in TS1 is comparatively small (P–Au–Ph = 171°). For the TSs at the right side of the two profiles, both TS2 (P–Au–Cl = 107°), and TS4 (P–Au–vinyl = 118°) show a large alteration from 180° . It is also interesting to note the different Au–Sn distances in the transition states. In TS3 (2.780 Å) and TS4 (2.783 Å), the Au–Sn distance clearly indicates a covalent bond (sum of the covalent radii is 2.75 Å). In TS1, this distance (2.974 Å) clearly indicates a somewhat weaker interaction.⁹ Finally in TS2 the distance is much longer (3.403 Å) although still shorter than the sum of vdW radii (3.83 Å), supporting at most an extremely weak indication. These distances point to very different orbital implications of the gold fragment at the initial interaction of the reagents in the two pathways.

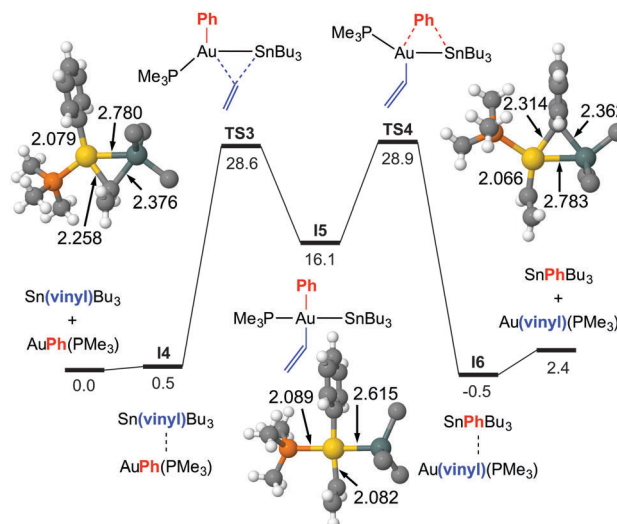


Fig. 2 Calculated Gibbs energy profile in THF (kcal mol⁻¹ at 323 K and $p = 301$ atm, bond distances in Å), for the rearrangement of [AuPh(PMe₃)] and Sn(vinyl)Bu₃ into [Au(vinyl)(PMe₃)] and SnPhBu₃. The *n*-Bu groups of the stannane have been simplified to C in the figure. Color code: C (gray), H (white), P (orange), Au (gold), Sn (dark green).



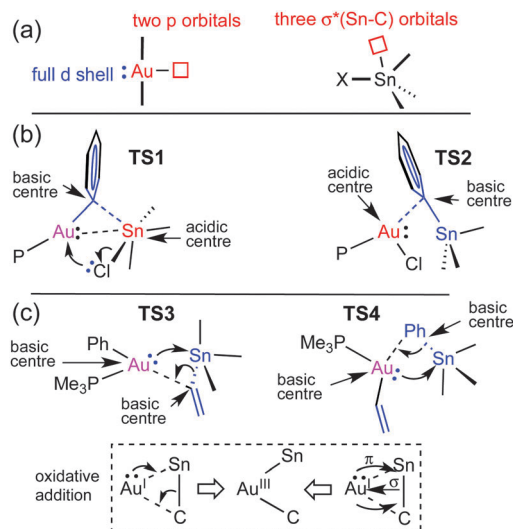


Fig. 3 Schematic orbital availability (a) and analysis of the electronic interactions involved in the transition states for exchange via: (b) transmetalation; (c) oxidative addition. Red is used for acidic centers, blue for basic, and pink for bifunctional. In the lower part of the figure two schematic representations of the electron redistribution leading to the gold intermediate **15** are shown. Both are similar although the one at the left indicates that the donating $\sigma(\text{Sn}-\text{C})$ orbital has more contribution of C, and the $\sigma^*(\text{Sn}-\text{C})$ accepting orbital has more participation of Sn.

Why are the two pathways so different? It is textbook knowledge that Sn can often expand its coordination number beyond four with common coordinating molecules.¹⁰ This can also happen with Au^{I} acting as a metalbase, as nicely shown by Bourissou in a specially designed bimetallic Au/Sn system where Sn becomes pentacoordinated by intramolecular interaction with gold as a donor ligand (experimental Au–Sn bond distance is 2.891 Å).¹¹ The orbital availability in the reagents examined here is schematically shown in Fig. 3a. The low energy unoccupied orbitals available for coordinative expansion in SnXBu_3 compounds are the three $\sigma^*(\text{Bu}-\text{Sn})$ orbitals (this availability is represented by a small square box). Their acceptor ability depends on the electronegativity of X (highly electronegative X groups will stabilize these orbitals and make them better acceptors) and on how much they are saturated by negative hyperconjugation with the four groups already bonded to tin.¹⁰ Hence, tin will be a much better acidic centre and better acceptor of a fifth ligand in SnClBu_3 than in $\text{Sn}(\text{vinyl})\text{Bu}_3$ because vinyl produces much higher hyperconjugation effect. On the other hand, the sp hybridized linear Au^{I} can expand its coordination number to 3 or 4 by involving its empty 6p orbitals in bonding (these are represented by a square box on Au in Fig. 3a). In addition, Au^{I} has the ability to show basicity (metalbasicity) by implicating electron density from its 5d closed shell orbitals in a donor–acceptor interaction with other acidic centres (represented as a lone pair in Fig. 3a, left). This metalbasicity increases with more electron donor groups on Au. Overall, depending on the ligands at Au the potential of our $[\text{AuX}(\text{PMe}_3)]$ complexes as metalbases should follow the trend vinyl > Ph > Cl, whereas the tendency of Au^{I} to increase its coordination number above 2 should be the opposite (Cl > Ph > vinyl).

The changes in acidity and basicity of the Au and Sn centres allow us to rationalize the structural variations observed in the transition states and, beyond that, the mechanistic switch observed. To this end the electronic interactions are schematically represented in Fig. 3b and c. For **TS2**, with a Cl ligand on gold, the metalbasicity of Au is expected to be the lowest, and its acidity the highest. Consistently, the interaction between the two fragments is established by electron donation from the Sn–Ph bond to an empty orbital in the gold centre, which becomes 3-coordinated, while the Sn atom remains 4-coordinated. The observation that the Au–Sn distance is shorter than the sum of vdW radii is not unexpected since the nature of all 3c2e electron deficient Au–C–Sn bridges should produce some degree of Au–Sn bond interaction not needing to invoke metallophilicity.¹² For **TS1**, which has the Cl ligand on Sn, this centre becomes very acidic, whereas the Au centre with a good donor Ph group is more basic than in **TS2**. Consequently, the Au–Ph bond attacks the acidic Sn, which becomes 5-coordinated. This donation from the Au–Ph bond increases the acidity of Au enough as to interact with a lone electron pair from the Cl ligand. Altogether, the metalbasicity of Au in **TS1** is likely higher than in **TS2**, which along with the higher acidity of Sn may contribute to increase the Au–Sn interaction and shorten the distance (Fig. 3b). To investigate in detail the Au–Sn interactions we carried out a second order perturbation theory analysis of the Fock matrices in the Natural Bond Orbital (NBO) basis (details in Table S6 of ESI†).¹³ For **TS1** (Fig. 4a) this analysis reveals an electron donation of 0.08 e from a 5d(Au) orbital to a $\sigma^*(\text{Sn}-\text{Bu})$ orbital with 85% Sn character shown in Fig. 4.

The structural features of **TS3** and **TS4** sharply differ from those of **TS1**, showing the group being transmetalated almost equidistant from Au and Sn, and displaying a strong Au–Sn bond. The respective highly donor hydrocarbyl group R (R = Ph, vinyl) attached to Sn saturates its potential acidity and the Sn–R moiety behaves as a nucleophile attacking the gold centre with the electron density of the $\sigma(\text{Sn}-\text{C}_\text{R})$ bond, more participated by

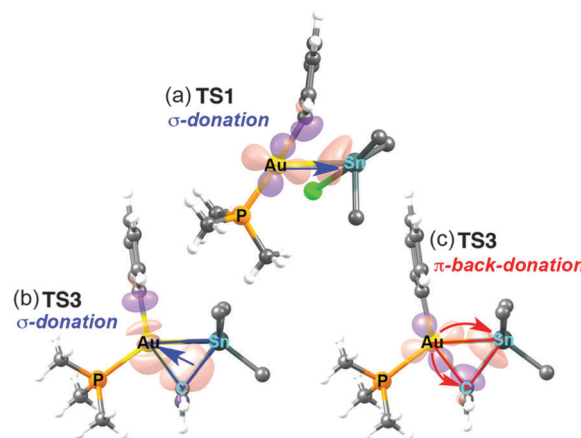


Fig. 4 Representation of the NBOs (isovalue = 0.09) involved in: (a) the donation from 5d(Au) to $\sigma^*(\text{Sn}-\text{C}_\text{Bu})$ in **TS1**; (b) the donation of the Sn– C_{vinyl} bond to the Au– C_Ph unit in **TS3**; and (c) the back-donation from Au to the Sn– C_{vinyl} bond in **TS3**. A schematic representation of these interactions in blue (b) and red (c) is superimposed.



the C atom. This leads to an electronically enriched 3-coordinated Au^I bearing two hydrocarbyl groups, which markedly enhances its metalbasicity from the 5d(Au) orbitals. In fact, this higher basicity not only favours the interaction with the empty $\sigma^*(\text{Sn}-\text{C}_R)$ orbital of the bridging group (Fig. 3c), but also weakens the Sn–C_R bond, eventually leading to the oxidative addition product **I5** (Fig. 2).

The NBOs in Fig. 4b and c confirm that there are direct donor–acceptor interactions orbital interaction between the two metal centres in **TS3**. This analysis can be decomposed into donation and back-donation components. The donation (Fig. 4b) consists in the σ -bond donation from a hybrid sp bonding orbital of the Sn–C_{vinyl} bond, which has 21% Sn and 79% C_{vinyl} character, to an empty natural bond orbital constituted mainly by the 6s orbital of Au (78%) and a hybrid sp orbital (22%) from the C_{Ph} (Fig. 4b). This interaction eventually results in the formation of the Au–vinyl bond in **I5**. On the other hand, the back-donation component (Fig. 4c) involves an electron donation of 0.17e from a 5d(Au) orbital to an anti-bonding orbital of the Sn–C_{vinyl} bond, which has a 79% Sn and 21% C_{vinyl} character. This interaction eventually results in the formation of the Au–Sn bond in **I5**. Based on the degree of implication of the 5d(Au) electron density (starting from no implication in **TS2** to small implication in **TS1** and large implication in **TS3**) we can say that it is mostly the increasing metalbasicity of Au^I that eventually leads to make oxidative addition accessible. Overall, the combination of donation and back-donation components is perfectly consistent with the classical image of a concerted oxidative addition of a X–Y moiety to a metal atom M, where 2 e of the X–Y bond to be broken and 2 e of the metal to be oxidized are shared to form two new X–M and M–Y bonds in a *cis* arrangement (Fig. 3, bottom). A similar pathway for the hypothetical oxidative addition of Sn(vinyl)H₃ to linear Pd(0) complexes was proposed by Matsubara.¹⁴

To our knowledge, this is the first time that the oxidative addition of a Sn–C bond to gold has been proposed. The Au^{III} complexes bearing Au–Sn bonds reported to date have been obtained by oxidative addition of a fairly weak Sn–Sn bond to gold(I).^{15,16} It is worth mentioning that experimentally we do not detect any Ph–vinyl coupling product by NMR, and only traces by GC. This coupling would require the Ph and vinyl groups to achieve a *cis* disposition, either directly from the oxidative addition, or by isomerization of **I5** to any of the two possible *cis*-C,C isomers. Calculations show that *cis*-Ph/vinyl *trans*-Ph/Sn isomer (the other *cis*-C,C isomer is expected to have very similar energy) is 8.2 kcal mol^{–1} less stable than the *trans* intermediate **I5**, and the calculated reductive elimination barrier to give Ph–vinyl is prohibitively high (*ca.* 44 kcal mol^{–1}, see ESI† for details).

Considering the reluctance of Au catalysts to participate in processes that require a difficult oxidation to Au^{III}, the accessibility of this oxidative addition mechanism is noteworthy, and deserves some comment. Thinking routinely of an oxidation state Au^{III} for **I5** we would infringe the rules to assign oxidation states to a metal. Obeying the formalism, the metal–metal bonds should not count, and gold in **I5** should be assigned Au^{II}. This reflects

that Au–Sn bonds make gold more electron rich (less “oxidized”) than, for instance, M–X or M–R bonds. For this reason, the oxidative addition process found here is more accessible than those leading to “more authentic” Au^{III} complexes, from which C–C reductive elimination is fast.¹⁷ These considerations help to understand why this Au^{III} is more accessible, but also less prone to afford coupling products.

In summary, we find that the Sn/Au transmetalation is very much influenced by the acidity of the tin centre and the metalbasicity of the gold centre. When electron donor groups on tin quench the acidity of the low-lying $\sigma^*(\text{Sn}-\text{C}_{\text{Bu}})$ orbitals by hyperconjugation and the aurobasicity increases in the TS, the transmetalation switches from the classical bridge mechanism to an oxidative addition pathway. This mechanism becomes effective by participation, as acceptor of the electron density from gold, of the $\sigma^*(\text{Sn}-\text{C}_R)$ orbital of the group being transmetalated.

This work was supported by the Spanish MINECO (grants CTQ2013-48406-P, and CTQ2014-52974-REDC) and the Junta de Castilla y León (grant VA256U13).

Notes and references

- Mechanistic studies on transmetalation involving Sn: (a) C. Cordovilla, C. Bartolomé, J. M. Martínez-Ilarduya and P. Espinet, *ACS Catal.*, 2015, **5**, 3040; (b) P. Espinet and A. M. Echavarren, *Angew. Chem., Int. Ed.*, 2004, **43**, 4704–4734; (c) M. H. Pérez-Temprano, A. Nova, J. A. Casares and P. Espinet, *J. Am. Chem. Soc.*, 2008, **130**, 10518; (d) M. H. Pérez-Temprano, A. M. Gallego, J. A. Casares and P. Espinet, *Organometallics*, 2011, **30**, 611.
- General review on transmetalation in bimetallic systems: M. H. Pérez-Temprano, J. A. Casares and P. Espinet, *Chem. – Eur. J.*, 2012, **18**, 1864.
- (a) J. delPozo, D. Carrasco, M. H. Pérez-Temprano, M. García-Melchor, R. Álvarez, J. A. Casares and P. Espinet, *Angew. Chem., Int. Ed.*, 2013, **52**, 2189; (b) J. delPozo, J. A. Casares and P. Espinet, *Chem. Commun.*, 2013, **49**, 7246.
- (a) J. J. Hirner, Y. Shi and S. A. Blum, *Acc. Chem. Res.*, 2011, **44**, 603; (b) Y. Shi, S. M. Peterson, W. W. Haberaecker and S. A. Blum, *J. Am. Chem. Soc.*, 2008, **130**, 2168.
- Y. Chen, M. Chen and Y. Liu, *Angew. Chem., Int. Ed.*, 2012, **51**, 6181.
- M. Joost, P. Gualco, S. Mallet-Ladeira, A. Amgoune and D. Bourissou, *Angew. Chem., Int. Ed.*, 2013, **52**, 7160.
- A. Ariafard, N. A. Rajabi, M. J. Atashgah, A. J. Canti and B. F. Yates, *ACS Catal.*, 2014, **4**, 860.
- Details are given in ESI†.
- For the Sn/Au transmetalation between [AuCl(AsMe₃)] and Sn(Naph)Me₃ a metal–metal interaction with Au–Sn distance 2.904 Å in the rate determining TS was calculated (ref. 3).
- C. Elschenbroich, *Organometallics*, Wiley-VCH Verlag GmbH&Co. KGaA, Weinheim, 3rd edn, 2006.
- P. Gualco, T. P. Lin, M. Sircoglou, M. Mercy, S. Ladeira, G. Bouhadir, L. M. Pérez, A. Amgoune, L. Maron, F. P. Gabbaï and D. Bourissou, *Angew. Chem., Int. Ed.*, 2009, **48**, 9892.
- J. delPozo, E. Gioria, J. A. Casares, R. Álvarez and P. Espinet, *Organometallics*, 2015, **34**, 3120.
- E. D. Glendening, J. K. Badenhoop, A. E. Reed, J. E. Carpenter, J. A. Bohmann, C. M. Morales, C. R. Landis and F. Weinhold, *NBO 6.0*, Theoretical Chemistry Institute, University of Wisconsin, Madison, 2013.
- T. Matsubara, *Organometallics*, 2003, **22**, 4286.
- N. Lassauque, P. Gualco, S. Mallet-Ladeira, K. Miqueu, A. Amgoune and D. Bourissou, *J. Am. Chem. Soc.*, 2013, **135**, 13827.
- Reviews about transition metal–tin chemistry: (a) D. Agustin and M. Ehses, *C. R. Chim.*, 2009, **12**, 1189; (b) M. S. Holt, W. L. Wilson and J. H. Nelson, *Chem. Rev.*, 1989, **89**, 11.
- W. J. Wolf, M. S. Winston and F. D. Toste, *Nat. Chem.*, 2014, **6**, 159.

